17^{th} World Conference on Earthquake Engineering, 17WCEE
Sendai, Japan - September 13th to 18th 2020

MONOTONICALLY COMPRESSIVE STRESS-STRAIN MODEL OF ULTRA-HIGH-STRENGTH REBAR CONSIDERING BUCKLING

A. Zhou [(1)], Y. Sun [(2)], T. Takeuchi [(3)], M. Jia [(4)], P. Luo [(5)]

[(1)] *Ph.D. Student, Graduate School of Engineering, Kobe University, aixin1031@gmail.com*
[(2)] *Professor, Graduate School of Engineering, Kobe University, sun@person.kobe-u.ac.jp*
[(3)] *Assistant Professor, Graduate School of Engineering, Kobe University, takeuchi_t@person.kobe-u.ac.jp*
[(4)] *Master Student, Graduate School of Engineering, Kobe University, jiamian940911@yahoo.co.jp*
[(5)] *Ph.D. Student, School of Civil Engineering, Southwest Jiaotong University, pengjunluo1988@gmail.com*

Abstract

Due to their superior physical and mechanical properties, ultra-high strength (UHS) reinforcement rebars (with yield stress over 1000MPa) have recently found wider and wider applications in high earthquake-resistant structures and high-resilient concrete reinforced (RC) components as longitudinal reinforcement. Buckling of longitudinal rebars in RC beams and columns is one of the important issue needed to be addressed when designing and evaluating seismic properties of concrete structures located in earthquake-prone zones such as Japan and China because the buckled rebars will decrease their axial load-resisting capacity, initiating the degradation in lateral load-carrying capacity and deformability of the RC components. To reasonably trace and accurately evaluate the post-peak seismic behavior of RC components, a complete compressive stress-strain model capable of capturing the post-buckling properties of the longitudinal rebars, both normal-strength and high-strength, is indispensable. While there have been numerous studies on the post-buckling behavior of reinforcement bars and several stress-strain models have been proposed in the literature, the previous studies mainly focused on normal-strength rebars with yield stress ranging from 300 MPa to 500MPa, and the models have been developed based on the experimental results of bare rebar specimens. There have been few, if any, information on the post-buckling behavior of UHS rebars embedded in concrete, neither a reliable compressive stress-strain model that can reliably evaluate the post-buckling behavior of UHS rebars.

This paper presents information on the post-buckling behavior of UHS rebars with yield stress of as high as about 1400 MPa and a complete compressive stress-strain model for the UHS rebars embedded in RC columns. Based on the so-called DM model and the experimental results, the complete stress-strain model for UHS rebars was developed. To validate the proposed stress-strain model, twelve short concrete columns were tested under monotonic axial compression with the spacing of transverse normal-strength reinforcement and the concrete grade as primary experimental variables. Comparison between the experimental results and theoretical predictions by the proposed model has indicated that the proposed model can satisfactorily simulate the compressive load-deformation response of UHS rebars reinforced concrete columns with consideration of post-buckling behavior of UHS rebars.

Keywords: Ultra high-strength rebar, reinforced concrete column, buckling, complete stress-strain model.

1. Introduction

A large amount of seismic damage investigations has indicated that reinforced concrete (RC) components exposed to severely seismic loads are vulnerable to failure by longitudinal rebars buckling. Owing to the weak capacity of the buckled longitudinal rebars in resisting the axial deformations, the occurrence of the rebar buckling usually results in the reduction of the ductility and energy dissipation capacity of RC components under the combination of gravity and lateral loads during earthquakes. Therefore, it is of particular importance to accurately evaluate the post-peak deformation response of RC components. In the last decades, extensive studies have been carried out in an attempt to develop the relevant material stress-strain models that are capable of capturing the post-buckling behavior of longitudinal rebars. Papia et al. [1] proposed a criterion to evaluate the peak load of the longitudinal rebars of compressed RC components. They found that a single parameter, which is proportional to the ratio between the stirrup stiffness and the shear stiffness of longitudinal rebar, was fairly suitable for determining the buckling length of the rebars. Monti and Nuti [2] experimentally and theoretically studied the stress-strain relations of the compressed bare rebars by considering the inelastic buckling effects. It was found that the ratios between unsupported length to rebar diameter significantly affect the post-buckling behavior of compressed rebars. Gomes and Appleton [3] modified the Menegotto-Pinto cyclic stress-strain model of steel rebars and successfully applied the modified model to consider the effect of the inelastic buckling of the longitudinal rebars. Based on the Gomes-Appleton model, Yang et al. [4] introduced an average stress reduction coefficient to take into account the core concrete expansion effects on the buckling behavior of reinforcement rebars. Dhakal and Maekawa [5] used the well-known tensile response parameters in defining the compressive response of reinforcement rebars and proposed a simple and accurate compressive stress-strain model with general applicability. Massone and Moroder [6] investigated the effect of initial imperfection on the buckling behavior of rebars and proposed a compressive stress-strain model with the capability of capturing initial imperfection effects. Many other studies [7,8] with respect to longitudinal rebar buckling have also been reported, however, most of them only focused on the normal-strength reinforcement rebars with yield stress ranging from 300 MPa to 500MPa.

Compared to a large number of investigations on the buckling of normal-strength reinforcement rebars, the study on the UHS reinforcement rebars is, if any, very few. Hu et al. [9] experimentally investigated the buckling behavior of the UHS reinforcement rebars using the bare rebar specimens and proposed an empirical model to predict the stress-strain curves of compressed UHS reinforcement rebars. However, the proposed model has not been proved to be applicable to UHS reinforcement rebars embedded in RC components.

Due to their superior physical and mechanical properties, high-strength (HS) and ultra-high-strength (UHS) reinforcement rebars (with yield strength over 1000MPa) have been more and more widely adopted to the construction of high earthquake-resistant structures [10], and high resilient concrete columns [11] as well as walls [12]. The authors have experimentally verified that using SBPDN rebar, an UHS rebar with low bond strength, as longitudinal tensile and compressive reinforcement could assure sufficient drift-hardening capability to concrete columns and walls [11,12]. Meanwhile, the previous study also indicated that the lateral resistance of concrete walls reinforced by SBPDN rebars tended to decrease due to crushing of concrete in compressive zone and local buckling of SNPDN bars at so large drift levels as 3.0% [12]. Therefore, to more accurately evaluate the drift-hardening capability of concrete walls with SBPDN rebars, the complete compressive stress-strain relations for the UHS rebars embedded in RC columns are desirable. To this end, in the present study, a complete stress-strain model for UHS rebars was developed based on the so-called DM model and experimental results. Then, the proposed model was applied to evaluate the axial behavior of twelve short concrete columns tested under monotonic compression.

2. Proposal of Stress-Strain Model

2.1 Original Dhakal and Maekawa (DM) model

To simulate the bare rebar buckling and develop a relevant stress-strain model, a series of three-dimensional nonlinear finite element analyses using the fiber technique were conducted by Dhakal and Maekawa [5]. The finite element model was first validated using the experimental results reported by some other researchers and then used for the parametric investigation. The parametric analysis results indicated that the buckling behavior of bare bars was controlled by the coupled effect of yield stress and slenderness ratio (defined as the ratio of unsupported length to bare bar diameter) of rebars. Based on these results, an average monotonic compressive stress-strain model, whose general layout is illustrated in Fig. 1, was developed.

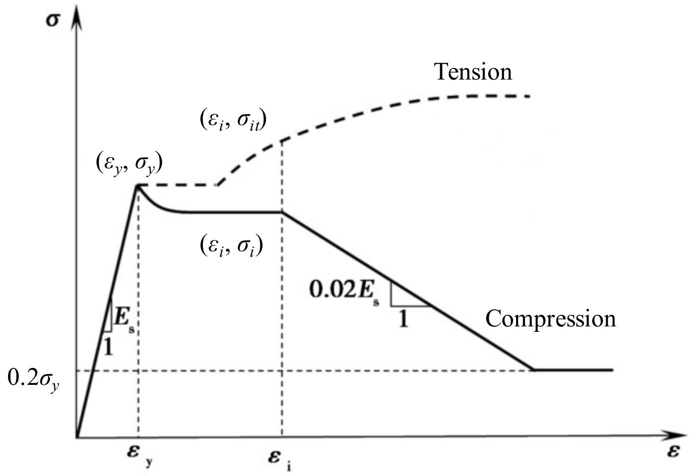

Fig. 1 – Schematic of DM stress-strain model

The linear elastic stage of the DM model is consistent with the tensile stress-strain curve and is defined as Eq. (1),

$$\sigma = E_s \cdot \varepsilon;\ \text{for } \varepsilon \leq \varepsilon_y \tag{1}$$

where ε_y is the yield strain, and E_s is the Young's modulus.

After the yield point (ε_y, σ_y), an intermediate point (ε_i, σ_i) is introduced to track the post-buckling behavior. Between the yield point and intermediate point, the average compressive stress-strain relationship is expressed as:

$$\frac{\sigma}{\sigma_t} = 1 - \left(1 - \frac{\sigma_i}{\sigma_{it}}\right)\left(\frac{\varepsilon - \varepsilon_y}{\varepsilon_i - \varepsilon_y}\right); \text{for } \varepsilon_y < \varepsilon \leq \varepsilon_i \tag{2}$$

in which σ_t and σ_{it} are the stresses of the tensile stress-strain curve corresponding to the current strain (ε) and the intermediate point strain (ε_i), respectively. The intermediate point (ε_i, σ_i) is determined by the expressions of Eqs. (3) and (4), which were obtained from the regression analysis for the data generated from the parametric study.

$$\frac{\varepsilon_i}{\varepsilon_y} = 55 - 2.3\sqrt{\frac{\sigma_y}{100}}\frac{L}{D}; \text{and } \frac{\varepsilon_i}{\varepsilon_y} \geq 7 \tag{3}$$

$$\frac{\sigma_i}{\sigma_{it}} = \alpha\left(1.1 - 0.016\sqrt{\frac{\sigma_y}{100}}\frac{L}{D}\right); \text{and } \sigma_i \ \geq 0.2\sigma_y \tag{4}$$

where L denotes the unsupported length and D denotes the bare rebar diameter. The coefficient α was used to account for the effect of different material hardening models. For the two most commonly used models, i.e., elastic-perfectly plastic model and linear hardening model, α was found to be 0.75 and 1.0, respectively. After the intermediate point (ε_i, σ_i), the average stress is assumed decreasing with a constant stiffness of $0.02E_s$ until $\sigma = 0.2\sigma_y$ and then keep constant as $0.2\sigma_y$.

2.2 Modified DM model for UHS rebars

Although the original DM model is applicable for a wide range of slenderness ratios and material properties, it is developed based on the results of normal-strength reinforcement rebars. It is noted that for the UHS rebars (with a yield stress of over 1400 MPa in this study), Eq. (3) is only viable for L/D values less than 5.5. In addition, the test results reported by Hu et al. [9] have indicated that the UHS rebars would buckle when the average stress less than the yield stress, which is significantly different from that for the normal-strength reinforcement rebars. Thus, the original DM model should be modified in order to suitable for UHS rebars.

Following the similar procedure used by Dhakal and Maekawa to develop the DM model, the intermediate points (ε_i, σ_i) for UHS rebars are determined by regression analysis for the test data obtained from the experiments on UHS rebars [9]. Fig. 2 shows the regression results for the determination of intermediate point coordinates. By doing so, for the UHS rebars, Eq. (3) and (4) are modified as follows,

$$\frac{\varepsilon_i}{\varepsilon_y} = 0.42 \cdot \beta^{-1.17} \tag{5}$$

$$\frac{\sigma_i}{\sigma_y} = \alpha(-0.98\beta^2 + 0.34\beta + 0.96) \tag{6}$$

in which β is defined as $0.01\sqrt{\frac{\sigma_y}{100}}\frac{L}{D}$. It is noted that both $\varepsilon_i/\varepsilon_y$ and σ_i/σ_y are less than 1.0 for larger β value, which implies that the UHS rebars with higher slenderness ratio are likely to buckle at the linear elastic stage. In such cases, the linear elastic stage of the DM model just continues to the buckle point (ε_b, σ_b) instead of the yield point (ε_y, σ_y), and the buckle point is consistent with the intermediate point determined by the means of Eq. (5) and (6).

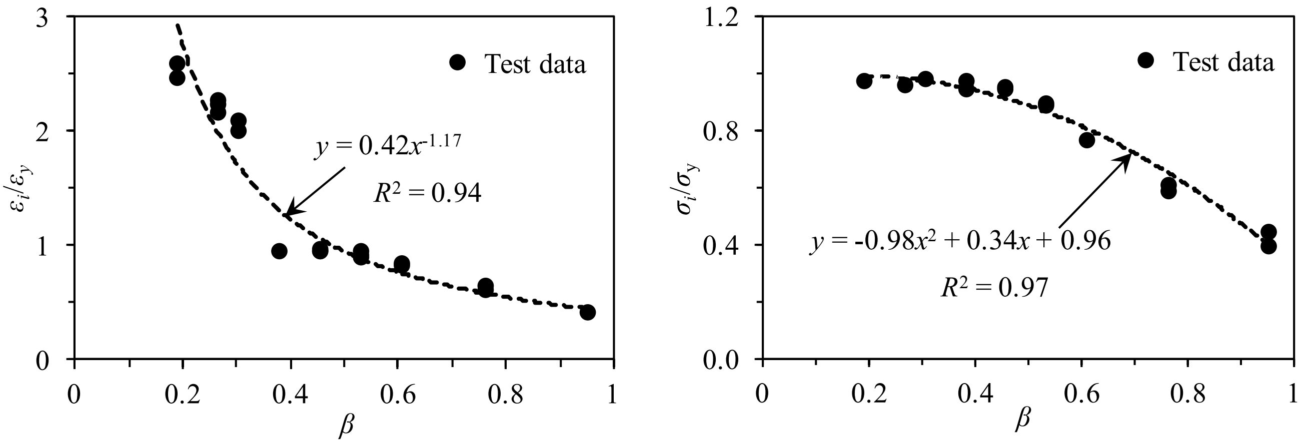

Fig. 2 – Determination of intermediate point coordinates for UHS rebars

After the intermediate point (ε_i, σ_i), for the cases of $L/D < 10$, the average stress is assumed linearly decreasing with a stiffness of $\alpha_1 E_s$, and the coefficient α_1 is determined by,

$$\alpha_1 = 0.231\,\beta - 0.032 \tag{7}$$

While, for the cases of $L/D \geq 10$, the average stress nonlinearly decreases following the expression of Eq. (8).

$$\frac{\sigma_i}{\sigma_y} = \alpha_2\left(\frac{\varepsilon}{\varepsilon_y}\right)^{\alpha_3} \tag{8}$$

where the coefficients α_2 and α_3, which were determined based on the regression analysis, can be calculated by the means of,

$$\alpha_2 = 0.30\beta^{-1.36} \text{ and } \alpha_3 = -0.48\beta^{-0.12} \tag{9}$$

Fig. 3 shows the comparison between the results obtained from the proposed stress-strain model and the experiments reported by Hu et al. [9]. As can be seen, the modified DM model is capable of regenerating the average stress-strain curves of bare UHS rebars under a monotonically compressive load.

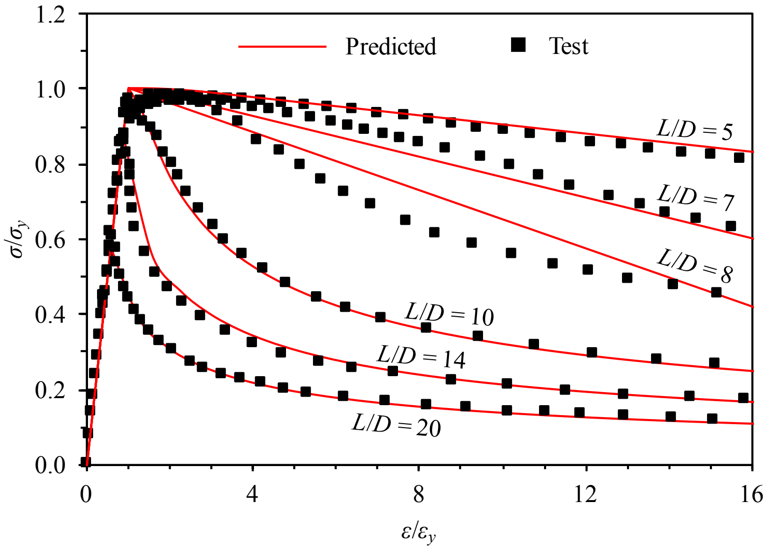

Fig. 3 – Comparison between the predicted and experiment stress-strain curves

2.3 Effect of core concrete expansion

It should be noted that the above-mentioned stress-strain models were developed based on the test results obtained from bare rebars. However, for the RC columns under compressive load, the core concrete tends not only to shorten lengthwise but also to expand laterally due to the Poisson effect. According to some previous investigations [3,4], the effect of core concrete expansion on the buckled rebars can be assumed as the distributed lateral force on acting on the longitudinal rebars. For simplicity, a correction coefficient as indicated in Eq. (10) can be introduced to consider the core concrete expansion effect on the average stresses of the longitudinal rebars,

$$\Omega = 1 - \frac{k_c K_0}{\sqrt{2}\sigma_y A_s} \ f(\varepsilon) \tag{10}$$

where k_c is the confinement effectiveness coefficient and K_0 is the parameter relating to stirrup arrangement, and both can be calculated according to the formulae reported in [4]. Since the buckled rebar would separate from the core concrete after onset of buckling, the strain functions $f(\varepsilon)$ with respect to different strain levels are determined by the means of,

$$f(\varepsilon) = \frac{1 - 0.667(\varepsilon/\varepsilon_i)}{2 - \varepsilon/\varepsilon_i} \cdot \frac{1 - \varepsilon}{2} \cdot \sqrt{\varepsilon} \text{ for } \varepsilon < \varepsilon_i \tag{11}$$

$$f(\varepsilon) = \frac{1 - \varepsilon}{6} \cdot \sqrt{\varepsilon_i} \text{ for } \varepsilon \geq \varepsilon_i \tag{12}$$

The average stresses of the buckled longitudinal rebars with considering the core concrete expansion can be obtained by multiplying the average stresses obtained from the modified DM model by the correction coefficient of Ω.

3. Application to experiment evaluation

3.1 Experimental program

To validate the proposed monotonically compressive stress-strain model for UHS rebar, a total of twelve columns, including six square columns and six circular columns, were fabricated and tested in this study. All columns are in height of 360 mm, with a cross-section side length of 150 mm for the square columns and a diameter of 150 mm for the circular columns. Fig. 4 shows the configurations of the test specimens. All the columns were reinforced by the UHS rebars (i.e., SBPDN). The nominal diameter of the SBPDN rebars was 12.6 mm. The hoops, which were made from SD295 deformed steel round rebars with a nominal diameter of 6.35 mm, were used to confine the core concrete and provide lateral restraints for the longitudinal rebars. The middle height regions of the columns were selected as the areas of interest to facilitate the investigation of buckling of longitudinal rebars. In the regions of concern, three different stirrup intervals, i.e., 50 mm, 75 mm, and 100 mm, were selected to yield the slenderness ratios of 4, 6, and 8, respectively. The stirrup interval decreased to 25 mm to ensure the longitudinal rebars would buckle at the middle height regions of the columns. The end plates, which were anchored on the longitudinal rebars using the bolt nuts, were used to facilitate the forming of the reinforcement cage. Both the end plates and bolt nuts would not be taken off and would be covered after casting concrete. After the columns were made, two steel jackets with the height of 95 mm were also mounted at two ends of each column to provide additional constraint for the concrete outside the concerned regions. By doing so, the columns were expected to be damaged only in the mid-height regions.

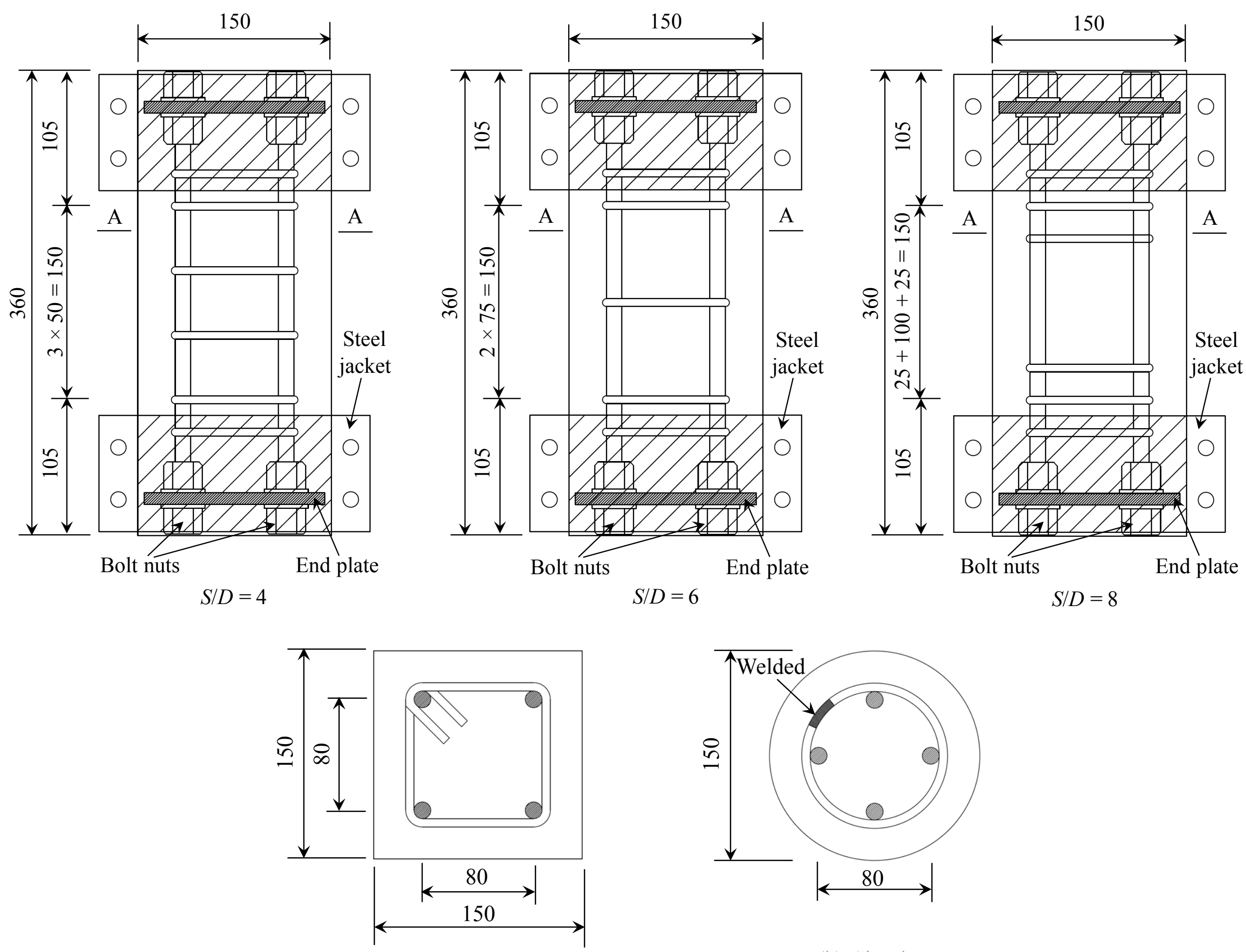

Fig.4 – Configurations of the test specimens (unit: mm)

According to the tensile coupon tests for three samples, the average values of Young's modulus (E_s), yield stress (f_y), yield strain (ε_y), tensile stress (f_u), tensile strain (ε_u), and the strain at starting point of hardening branch (ε_{sh}) were obtained and listed in Table 1.

Two different grades of ready-mixed concrete made of Portland cement and coarse aggregates with the maximum particle size of 20 mm were used for constructing the columns. Based on the test results from three cylinders 100 × 200 mm in dimensions at 28 days after casting, the average values of compressive strength, splitting tensile strength, Young's modulus, and peak strain are 43.4 MPa, 3.2 MPa, 27.5 GPa, 0.0025 for the normal-strength grade concrete (C40) and 70.7 MPa, 6.1 MPa, 33.9 GPa, 0.0025 for the high-strength grade concrete (C60). Table 2 summarizes the matrix of testing specimens, in which D is the diameter of longitudinal rebar, d is the diameter of stirrup rebar, S is the stirrup spacing, S/D is the slenderness ratio, and f_c' is the actual concrete compressive strength at the time of testing.

Table 1 – Material properties of steel rebars

Grade	E_s (MPa)	f_y (MPa)	ε_y (%)	ε_{sh} (%)	f_u (MPa)	ε_u (%)
SD295	191	400	0.21	1.52	523	20
SBPDN	212	1397	0.86*	/	1470	10

Note: * obtained from the 0.2% offset method.

Table 2 – Matrix of testing specimens

Specimens	Longitudinal rebar	Transverse stirrup	D (mm)	d (mm)	S (mm)	S/D	Concrete grade	f_c' (MPa)
S40-4	SBPDN	SD295	12.6	6.35	50	4	C40	50.1
S40-6	SBPDN	SD295	12.6	6.35	75	6	C40	50.1
S40-8	SBPDN	SD295	12.6	6.35	100	8	C40	50.1
S60-4	SBPDN	SD295	12.6	6.35	50	4	C60	76.9
S60-6	SBPDN	SD295	12.6	6.35	75	6	C60	76.9
S60-8	SBPDN	SD295	12.6	6.35	100	8	C60	76.9
C40-4	SBPDN	SD295	12.6	6.35	50	4	C40	50.1
C40-6	SBPDN	SD295	12.6	6.35	75	6	C40	50.1
C40-8	SBPDN	SD295	12.6	6.35	100	8	C40	50.1
C60-4	SBPDN	SD295	12.6	6.35	50	4	C60	76.9
C60-6	SBPDN	SD295	12.6	6.35	75	6	C60	76.9
C60-8	SBPDN	SD295	12.6	6.35	100	8	C60	76.9

Axially monotonic compression load was applied to the columns using a universal testing machine with a capacity of 2000 kN. Four linearly variable differential transformers (LVDTs) were used to measure the overall axial displacements. The tests were stopped when the axial shortening reached to 4% of the length of the specimen (i.e., average overall axial displacement of about 14.4 mm).

3.2 Load-displacement curves

To predict the load-displacement curves of the tested columns, the stress-strain constitutive model proposed by Sun et al. [13] was applied to simulate the axial behavior of confined concrete. The stress-strain relationship of the core concrete loaded under compression can be written as follow [13]:

$$f_c = \frac{AX + (B-1)X^2}{1 + (A-2)X + BX^2} f_{cc}' \tag{13}$$

where $X = \varepsilon_c / \varepsilon_{cc}$, f_{cc}' and ε_{cc} are the stress and strain of confined concrete at the peak point; $A = E_c / E_{sec}$, $E_c = (0.69 + 0.34\sqrt{f_c'})\times 10^5$ is the Young's modulus of concrete, $E_{sec} = f_{cc}'/\varepsilon_{cc}$ is the secant modulus at the peak; B is the parameter governing the slope of descending branch. The three parameters f_{cc}', ε_{cc}, and B are given as:

$$f_{cc}' = f_c' + 11.5\rho_h\sigma_{yh}(\frac{d'}{C})(1 - \frac{S}{2D_c}) \tag{14}$$

$$\frac{\varepsilon_{cc}}{\varepsilon_{cu}} = \begin{cases} 1 + 4.7(K-1), & K \le 1.5 \\ 3.35 + 20(K-1.5), & K > 1.5 \end{cases} \tag{15}$$

$$B = 1.5 - 0.017 f_c' + 1.6\sqrt{\frac{(K-1)f_c'}{23}} > 0.5 \tag{16}$$

in which f_c' is the actual concrete compressive strength at the time of testing (see Table 1); $\varepsilon_{cu} = 0.94(f_c')^{0.25}\times 10^{-3}$ is the strain of unconfined concrete at the peak stress point; $K = f_{cc}'/f_c'$ is the strength enhancement ratio of confined concrete; ρ_h, σ_{yh}, d', C, and D_c are the parameters related to the lateral hoops [13]. Note that $\rho_h = 0$ corresponds to the case of unconfined concrete and can be used to simulate the case of cover concrete.

For the test results, the load was measured from the load cell and the displacement was measured as the average value of four LVDTs. For the predicted results, the total load (N) was calculated by considering the contributions of cover concrete (N_{cov}), core concrete (N_{cor}), and longitudinal rebars (N_s) as the following expression,

$$N = N_{cov} + N_{cor} + N_s \tag{17}$$

where N_{cov} and N_{cor} are calculated using Eq. (13) to (16), N_s is calculated using the stress-strain model proposed in Section 2. The comparison results between the test and predicted axial load-displacement curves of all the tested columns are shown in Fig. 5 to Fig. 8. For comparison purposes, the axial load-displacement curves without considering longitudinal rebar buckling are also plotted. It is clearly shown that the proposed stress-strain model for considering the buckling of UHS rebars can track the load-displacement curves of square or circular RC columns with different concrete grades very well.

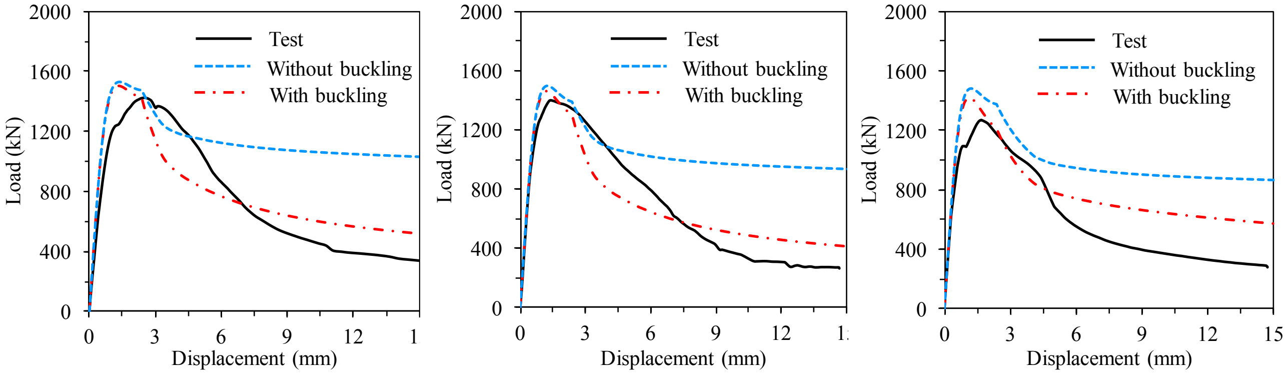

(a) S40-4 (b) S40-6 (c) S40-8

Fig.5 – Axial load-displacement curves of square specimens with C40 concrete

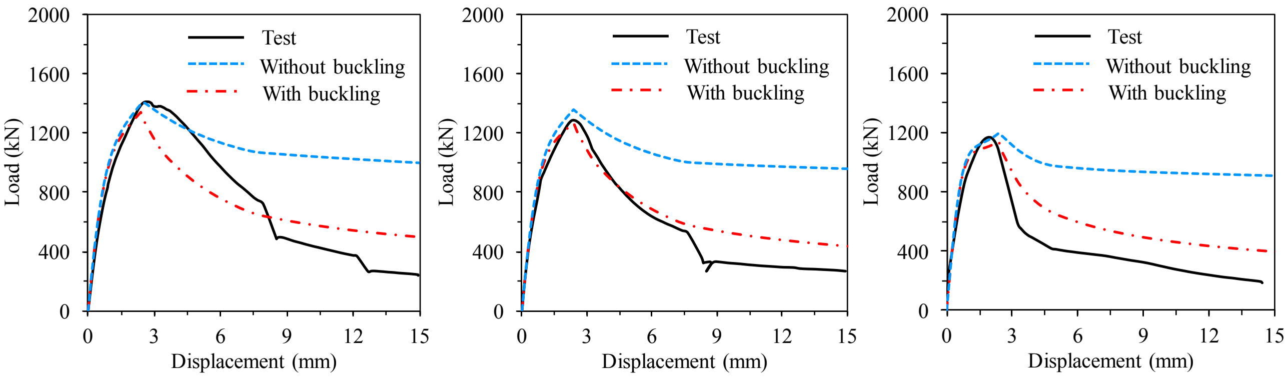

(a) C40-4 (b) C40-6 (c) C40-8

Fig.6 – Axial load-displacement curves of circular specimens with C40 concrete

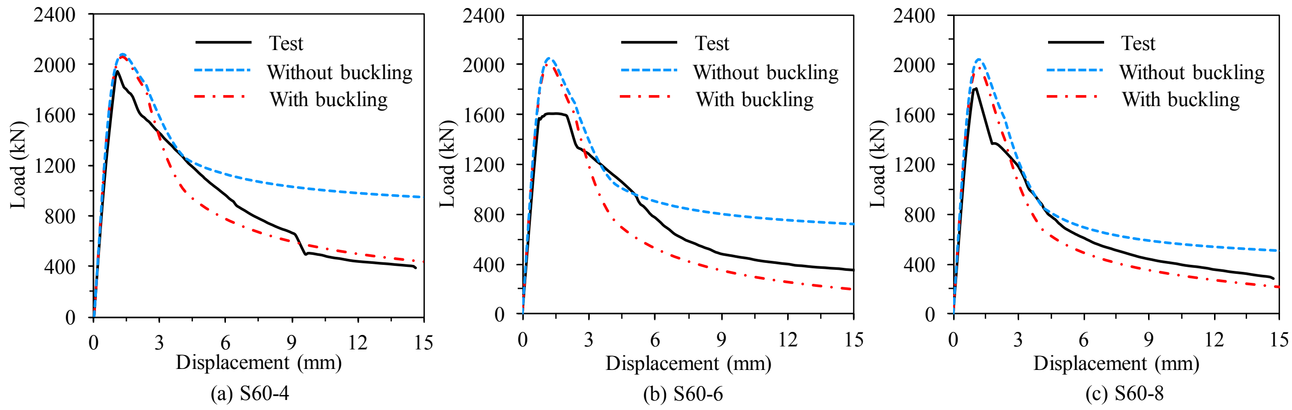

Fig.7 – Axial load-displacement curves of square specimens with C60 concrete

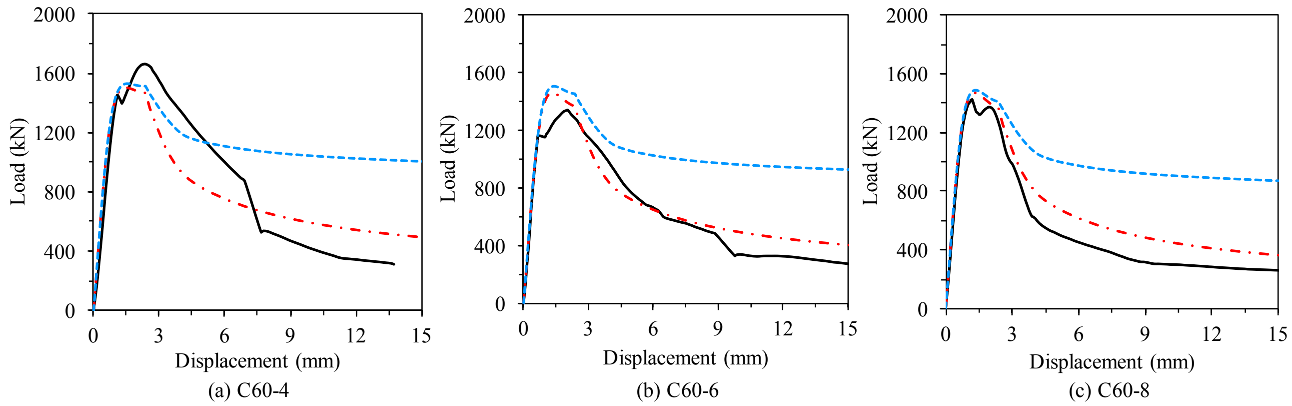

Fig.8 – Axial load-displacement curves of circular specimens with C60 concrete

4. Conclusions

To provide structural engineers a useful and powerful tool for evaluating the post-buckling behavior of RC components reinforced by UHS rebars, a monotonically compressive stress-strain model of UHS rebar considering buckling has been proposed. Comparisons with the previous tests have indicated that the proposed model is capable of regenerating the average stress-strain curves of bare UHS rebars under a monotonically compressive load. It has also been shown that the load-displacement curves based on the proposed stress-strain model agreed well with the test results generated from both square and circular stub columns fabricated using the concrete with different compressive strengths. These findings imply that the proposed stress-strain model provides structural engineering a useful and reliable tool to conduct reasonable design for RC components reinforced by UHS rebars considering the longitudinal rebar buckling.

5. Acknowledgements

This work was partially supported by JSPS KAKENHI No. 19H02289. Neturen Co. Ltd is greatly appreciated for providing the SBPDN rebars.

6. References

[1] Papia M, Russo G, Zingone G (1988): Instability of longitudinal bars in RC columns. *Journal of Structural Engineering*, 114(2), 445-461.

[2] Monti G, Nuti C (1992): Nonlinear cyclic behavior of reinforcing bars including buckling. *Journal of Structural Engineering*, 118(12), 3268-3284.

[3] Gomes A, Appleton J (1997): Nonlinear cyclic stress-strain relationship of reinforcing bars including buckling. *Engineering Structures*, 19(10), 822-826.

[4] Yang H, Jian B, Zhang X (2018): Modeling of buckled reinforcing bars including effect of lateral expansion of concrete core. *International Journal of Civil Engineering*, 16(9), 1005-1016.

[5] Dhakal RP, Maekawa K (2002): Modeling for postyield buckling of reinforcement. J*ournal of structural engineering*, 128(9), 1139-1147.

[6] Massone LM, Moroder D (2009). Buckling modeling of reinforcing bars with imperfections. *Engineering Structures*, 31(3), 758-767.

[7] Zong Z, Kunnath S, Monti G (2013): Material model incorporating buckling of reinforcing bars in RC columns. *Journal of Structural Engineering*, 140(1), 04013032.

[8] Akkaya Y, Guner S, Vecchio FJ (2019): Constitutive model for inelastic buckling behavior of reinforcing bars. *ACI Structural Journal*, 116(2), 195-210.

[9] Hu M, Han Q, Xu K, Du X (2019): Corrosion influences on monotonic properties of ultra-high-strength reinforcing steels. *Construction and Building Materials*, 198: 82-97.

[10] Lepage A, Tavallali H, Pujol S, Rautenberg J (2008): Towards earthquake-resistant concrete structures with ultra-high strength steel reinforcement. *14th World Conference on Earthquake Engineering*, Beijing, China.

[11] Sun Y, Cai G, Takeuchi T (2013): Seismic behavior and performance-based design of resilient concrete columns. *International Journal of Applied Mechanics and Materials*, 438, 1453-1460.

[12] Fujitani T, Sun Y, Takeuchi T, Wei C (2018): Study on effect of strength of rebars on the seismic performance of rectangular concrete walls. *Proceeding of Japan Concrete Institute*, 40(2), 313-318.

[13] Sun Y, Sakino K, Yoshioka T (1996): Flexural behavior of high-strength RC columns confined by rectilinear reinforcement. *Journal of Structure and Construction Engineering*, 486: 95-106.

